

ON QUENCH PROPAGATION, QUENCH DETECTION AND SECOND SOUND IN SRF CAVITIES

R. Eichhorn[#], D. Hartill, G. Hoffstaetter, and S. Markham

Cornell Laboratory for Accelerator-Based Sciences and Education, Cornell University
Ithaca, NY 14853-5001, USA

Abstract

The detection of a second sound wave, excited by a quench, has become a valuable tool in diagnosing hot spots and performance limitations of superconducting cavities. Several years ago, Cornell developed an oscillating super-leak transducer (OST) for these waves that nowadays is used world-wide. In a usual set-up, several OSTs surround the cavity, and the quench location is determined by trilateration of the different OST signals.

Convenient as the method is, there is a small remaining mystery: taking the well-known velocity of the second sound wave, the quench seems to come from a place slightly above the cavity's outer surface. We will present a model based on numerical quench propagation simulations and analytic geometrical calculations that helps explain the discrepancy.

INTRODUCTION

Many future linear accelerators rely on superconducting radio frequency (SRF) cavities to accelerate the particles. During the last decade, the advantages of SRF technology compared to normal conducting RF systems based on copper resonators have been broadly recognized. Early SRF cavities had low accelerating gradients, high RF losses and, being the most serious issue, a very unreliable performance reproducibility. State of the art SRF cavities have overcome these limitations: they reach high gradients and low losses, very close to the theoretical limit. Many of the advances in the field are due to a better understanding of the surface effects in SRF cavities, quench limits and contamination.

Today's SRF cavities undergo a sophisticated fabrication scheme which ensures a smooth and uniform surface. Despite precautions taken, it is still common for cavities to bear small (sub-millimeter) surface defects that impede cavity performance. These defects cause localized excess heating, eventually causing a quench to normal conductivity and limiting the cavity's performance.

One method of locating a defect involves using oscillating superleak transducers (OSTs [1]) to detect second sound waves emitted from the cavity. Second sound is a phenomenon observed in superfluid helium [2] wherein heat propagates as a wave with properties comparable to that of a classical sonic wave. The speed of the second sound depends somewhat on the parameters of the fluid, but is almost a constant of 20 m/s, within the temperature range of 1.6 to 2 K.

By measuring the time of arrival of the 2nd sound wave-

front at the detectors relative to the time of the RF field collapse, the distance between each transducer and the defect heated region may be calculated. This information is used in trilateration the defect location using the well-know propagation velocity of the sound wave. A common problem in the trilateration is that the source of the second sound wave seems to be located above the cavity surface, giving rise to various theories as the propagation speed of the wave would have to be larger than published data if it propagated from the defect through helium, starting at the time of field-collapse[3-5].

Within this paper we will elaborate on two mechanisms that explain the early arrival of the wave. We will present results from dynamic heat transport calculation through the niobium which includes the ring-down of the RF field inside the cavity after the onset of the quench. Furthermore, this paper will describe how heat propagation in the niobium can contribute to the quench signal propagation and to the misinterpretation of the quench location.

MODEL SPECIFICATION

A MATLAB computational model is used to investigate the time dependent dynamics of the SRF cavity with a known defect under medium RF field conditions. We were particularly interested in the potential disparity between the time of the excitation of a second sound wave on the Nb-HeII interface and the time where losses in stored energy of the SRF system become significant. Our model has two arbitrarily chosen parameters: one being the heat flux level at which a significant and detectable amplitude of the second sound wave is generated and the other being the drop in RF power at which a quench is realized. We will discuss our choice of parameters below and allow the readers to draw conclusions using different values for these parameters.

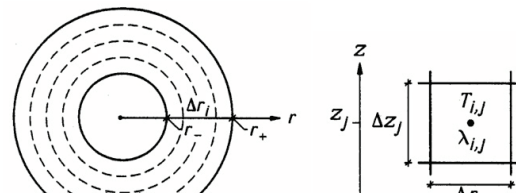


Figure 1: Discretization used for calculating the heat propagation through the niobium. The coordinate system is centred around the defect, reducing the calculations to a quasi-2D problem.

Our model considers a niobium cavity with a surface defect which is characterized by normal conducting resistivity. The remainder of the cavity is initially in the superconducting state, and undergoes thermal breakdown. The basic mechanics of the simulation assumes a cylindrically symmetrical geometry, centered around the defect, as depicted in Fig. 1. This reduces the problem to a quasi two-dimensional problem. The basic methodology has been used by others, too ([4] with more references in [6].

The specifics of our model are based on canonical computational methods for heat conduction as published in [7]. The model separates a cylindrical disk of niobium into mesh elements, each with a different temperature which result in different physical properties. The model then iteratively computes heat transfer and ohmic heat dissipation into each of the relevant mesh elements. The choice of time step to ensure numerical stability is chosen according to canonical methods described in [8]. The stipulation on the time step is:

$$\Delta t < \frac{C_{ij} 2\pi r_i \Delta r \Delta z}{K_{i-1,j} + K_{i+1,j} + K_{i,j-1} + K_{i,j+1}} \forall i, j$$

where C_{ij} is the specific heat capacity at cell (i,j) and $K_{i-1,j}$ is the thermal conductance between cell (i, j) and cell $(i - 1, j)$, etc. These were calculated like

$$K_{i,j-1} = \frac{2\pi r_i \Delta r}{\Delta z (\kappa_{i,j-1} + \kappa_{i,j}) / 2}$$

and

$$K_{i-1,j} = \Delta z \cdot \left(\frac{\ln(r_i / r_{i-0.5})}{2\pi \kappa_{i-1}} + \frac{\ln(r_i / r_{i+0.5})}{2\pi \kappa_i} \right)^{-1}$$

where $\kappa_{i,j}$ is the temperature dependent thermal conductivity of cell (i,j) and Δr and Δz are the radial and lateral step sizes, respectively. In order to ensure the time step was less than this quantity, we calculated the quantity for each cell in the mesh, found the minimum and multiplied that value by some constant less than one.

The resistivity of the non-defective superconducting portion of the cavity is characterized solely by residual resistance and BCS resistivity, while the resistivity of the defect is characterized by joule heating according to the skin effect equation. For the BCS resistance we followed a model describe in [9], given by

$$R_{BCS} = (2.78 \cdot 10^{-5} \Omega) \frac{v^2}{t} \ln \frac{148t}{v} \exp - \frac{1.81g(t)}{t}$$

with the parameters (reduced temperature, normalized frequency and energy gap of the superconductor):

$$t = \frac{T}{T_c}; v = \frac{f}{2.86GHz}; g(t) = \sqrt{\cos \frac{\pi t^2}{2}}$$

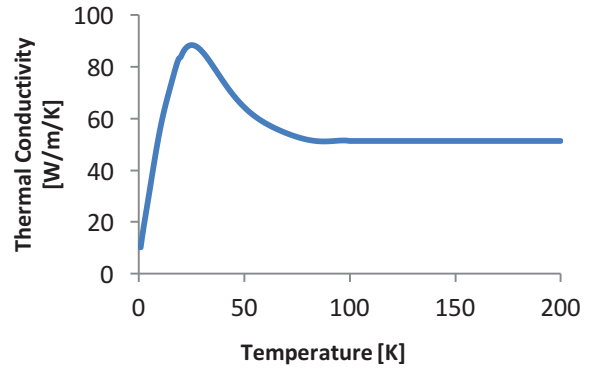


Figure 2: Thermal conductivity of the niobium used in our calculation (data from [10]).

The authors are well aware of the fact that various modifications of this formula exist with slightly different parameters. However, the results we derived and report below do not rely on a specific expression for the BCS resistance.

Some of our calculations were done including the Kapitsa resistance of the niobium-helium interface. We found that the inclusion of the resistance changed the results by less than 1%, indicating that the Kapitsa resistance is not a significant contributor to the thermal dynamics of an RF quench.

Heat capacity and thermal conductivity of the Niobium were calculated according to empirical numerical fits by [10] and [11]. The fits are plotted in Fig. 3 and Fig. 4.

In theory, there exists no lower threshold for the second sound wave: the smallest change in temperature should be able to propagate through the helium. However, experiments indicate that the detection of the second sound wave may have a lower limit. To make a conservative assumption, we chose that a second sound wave with a detectable amplitude is triggered when the heat flux is greater than 1.5 W/cm^2 . This choice was based on the heat flow through the helium becoming turbulent. It certainly represents a very high heat flux and more realistic values might be an order of magnitude lower. How this would impact our conclusions will be discussed below.

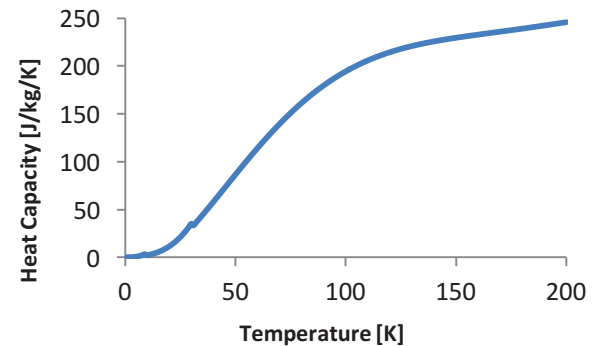


Figure 3: Heat capacity as a function of the temperature, as found in [11].

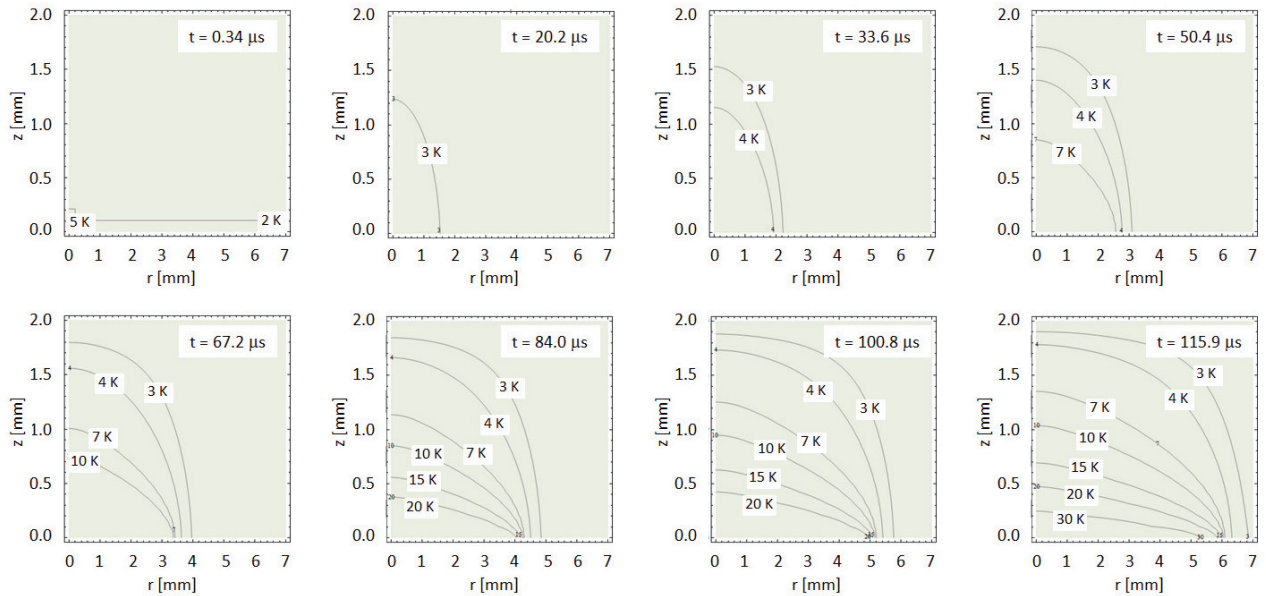


Figure 4: Visualization of the quench spot and the heating as it expands in r and z direction. The heating spot is located in the lower left corner.

The simulation was run using the formulae given and the material parameters plotted above for the mesh size as specified. We used typical quench conditions with a magnetic field strength of 0.126 T. The initial temperature of the niobium was set below the lambda point of helium at 2 K. A 0.2 mm normal conducting defect was introduced at the center. A visualization of the quench dynamics as calculated is shown in Fig. 4.

We found that the noticeable loss in stored energy (which we assumed to be a 2% change in stored energy) occurs after 1.1×10^{-4} s while the second sound wave (under our conditions) is excited already after 8.0×10^{-5} s. As a result (under the given assumptions) the second sound wave is excited 30 μs before the quench is noticeable on the RF side. This translates into a distance of more than 1 mm and explains the findings why the second sound wave seems to come from a location above the surface.

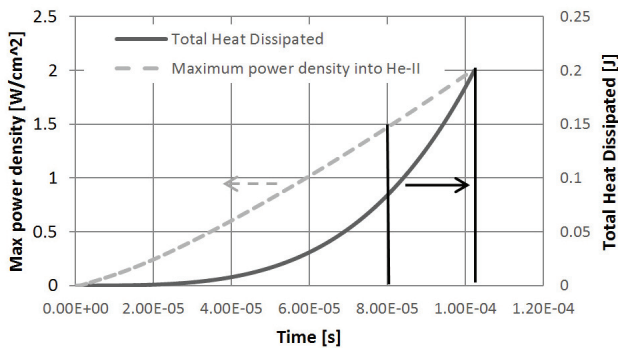


Figure 5: Temporal evolution of two simulation outputs. The gap represents the delay between second sound wave triggered and the quench detection.

These results are shown in fig. 5 and they allow the evaluation of the effects of the choice of the free parameters: if you assume the second sound wave is excited at a heat flux level of 0.15 W/cm^2 (which the reader might find more reasonable) the time difference between the second sound wave excitation and the RF quench detection becomes $100 \mu\text{s}$ which then explains the spatial discrepancy of almost 5 mm, more typically found in experiments. If one considers an RF detection limit of greater than 2% the time delay between the two incidents increases and decreases when lowering the limit to 1%. However, it should be noted that the dependency from that trigger level is less sensitive time-wise as the curve has a steeper slope.

INDIRECT HEAT PROPAGATION

Our model so far is able to explain why the quench location gained from trilateration seems lay above the cavity surface, but it cannot explain why the trilateration circle often do not intersect.

Figure 6 illustrates the basic geometry of the model we developed to explain this finding. For simplicity, the niobium is assumed to be planar, in thermal contact with helium-II and the OST is placed at a distance R from the defect under an angle θ from the normal.

Naively, one would assume a signal propagates to the OST in $\Delta t = R/v_{SS}$, where v_{SS} is the velocity of second sound in helium-II. However, if the signal also propagates across the niobium, following the path shown in Fig. 6, it will arrive at the OST in

$$\Delta t = \frac{x_0}{v_{Nb}} + \frac{\sqrt{(R \sin \theta - x_0)^2 + (R \cos \theta)^2}}{v_{SS}} \quad (1)$$

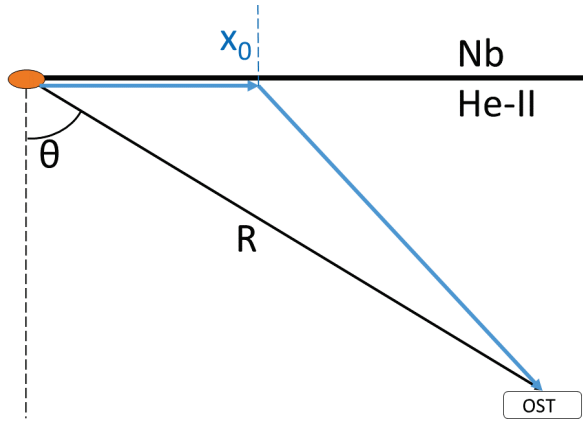


Figure 6: OST setup. Under certain conditions, the heat signal can arrive at the OST faster by travelling along the niobium and then propagating through the helium.

For large angles θ , this can be faster than the direct signal propagation if the propagation in niobium is faster than in Helium ($v_{Nb} > v_{SS}$). Minimizing this equation with the constraints $0 < x_0 < R \sin \theta$, we can find the value of x_0 that minimizes Δt , from which we can infer the time it takes for the fastest signal to reach the OST. The fastest propagation signal is simply $\Delta t = R/v_{SS}$ unless the angle reaches the threshold:

$$\theta_{thresh} = \arctan\left(\frac{v_{SS}}{\sqrt{v_{Nb}^2 - v_{SS}^2}}\right) \quad (2)$$

The full solution to the propagation problem, then, is:

$$\Delta t(\theta \leq \theta_{thresh}) = \frac{R}{v_{SS}} \quad (3)$$

$$\begin{aligned} \Delta t(\theta > \theta_{thresh}) &= \frac{R \sin \theta}{v_{Nb}} \\ &+ R \cos \theta \sqrt{\frac{1}{v_{SS}^2} - \frac{1}{v_{Nb}^2}} \end{aligned} \quad (4)$$

Solving the thermal diffusion equation in Niobium analytically [12], one finds a propagation speed of $v_{Nb} = 69$ m/s for normal conduction niobium. Figure 7 plots $\Delta t(\theta)$, given by (4) using this velocity.

Depending under which angle the OSTs are in relation to the initial quench location, a significant propagation time disparity can exist. The situation gets more serious, if one assumes the thermal diffusion velocity of superconducting niobium, being 800 m/s. As a result, the onset angle according to (2) gets smaller and the disparity increases, significantly

To test under which speed the heat propagates inside the niobium, and whether the diffusivity speed of normal or of superconducting niobium applies, we conducted a numerical simulation, described below.

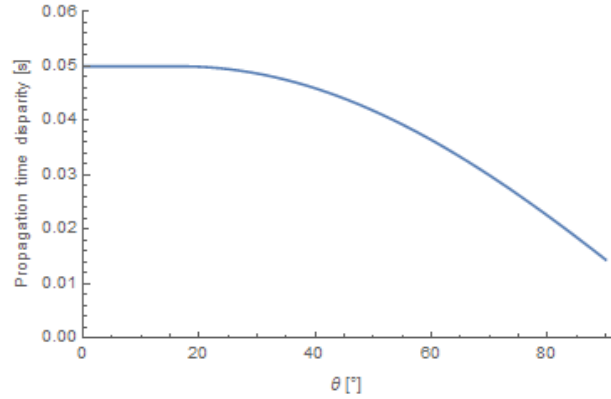


Figure 7: Propagation time (s) as a function of θ ($R = 1$ m, $v_{SS} = 20$ m/s, $v_{Nb} = 69$ m/s).

Computational Setup

In order to numerically simulate time dependent quench dynamics, we use our Matlab program Sherry, as described above. For each time step, Sherry calculates the heating on the RF surface of the cavity, the thermal diffusion through the niobium based on the heat capacity and the thermal conductivity, as well as the heat flux between the niobium and helium-II. Figure 8 shows the radius of normal conducting region on the RF side of the niobium as a function of time. Also shown in fig. 8 is the size of the outer surface of the niobium exceeding the heat flux of 1.5 W/cm², which starts to grow at $t = 80$ μ s.

As can be seen, the propagation speed of the heat on the inner surface and the expansion of the outer heat zone are constant and identical. The expansion speed we found in our calculation was 67 m/s, which agrees quite closely the previously cited value of 69 m/s. From that one can conclude that the quench signal propagation inside the niobium follow the thermal diffusivity law of the normal conducting state.

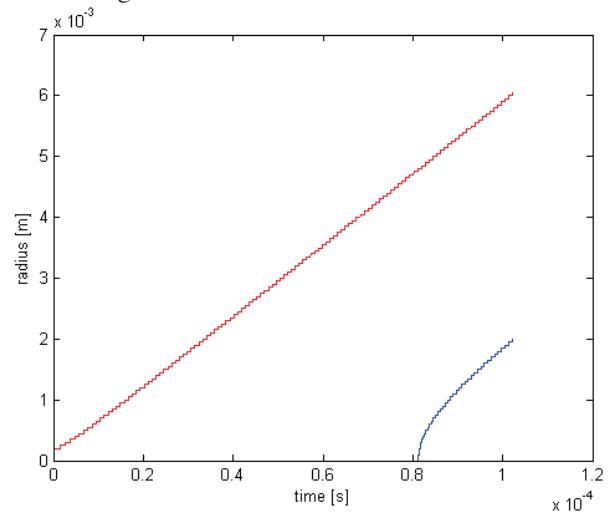


Figure 8: Radius of the normal conducting region on the RF side of the cavity (red curve) and the size of the heated zone (as defined in the text) on the outside (blue).

Results

Using the difference between the naïve assumption of propagation time, $\Delta t = R/v_{SS}$, and our full solution in (3) and (4), we can predict the disparity between the real defect location and the computed defect location using the OST trilateration method.

As an example, one can take a simple geometry with three OSTs set up in an equilateral triangle centered on the defect. Each OST is at $R = 0.5$ m and an angle θ from the defect. Using canonical trilateration methods with a sphere radius of $v_{SS}\Delta t(\theta)$, one can calculate the expected location of the defect that triggered the quench. A two dimensional analogue of this setup is depicted in Fig. 9.

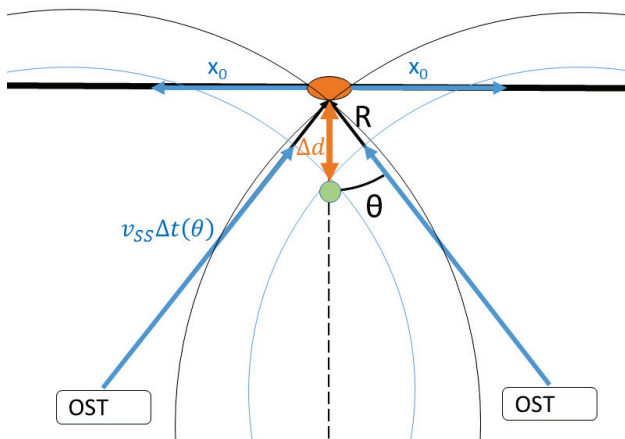


Figure 9: Two dimensional analogue example setup. The distance between the red and green intersection points is Δd , the error in reconstructing the quench location when only considering second sound.

The black circles represent the true distance from the OSTs to the defect. Their intersection is the true location of the defect. The blue circles represent the predicted location of the defect using pure second sound propagation, only. Their intersection is marked by the green circle, which represents the predicted location of

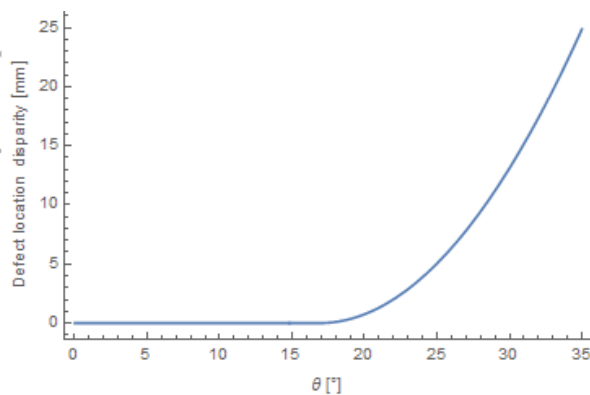


Figure 10: Defect location disparity as a function of θ , based on our specified setup.

the defect. Fig. 10 calculates the error in position resulting from neglecting heat propagation through the niobium $\Delta d(\theta)$ as a function of the angle. As can be seen, at angles greater than 20° the dislocation can be several millimetres- which is what experimenters observed.

CONCLUSION

Our calculations have revealed two potential sources for the systematic errors introduced when trying to localize quenches using OST second sound methods in superconducting cavities.

We found that the rate of power dissipation at the Nb-HeII interface reaches a level that would trigger a second sound wave potentially before a noticeable loss in the stored energy of the cavity occurs. If one defines the time of the quench as the moment the cavity energy noticeably decays and uses that to try to localize the quench inducing defect, this time may disagree under conservative assumptions with the time the second sound wave was actually excited by at least $30 \mu s$. This would correspond to a systematic error on the order of 1 mm assuming the speed of second sound is about 20 m/s.

Using purely geometrical arguments, we found an explanation for the disparity between defect location and OST quench detection predictions, if the heat propagates through the niobium faster than it propagates through the helium. We conducted numerical heat propagation calculations that found the signal velocity through niobium to be close to the theoretical thermal diffusivity value in normal conducting niobium, 69 m/s.

We think the main contributors to this disparity in second sound quench detection have now been identified.

ACKNOWLEDGMENTS

This work has been supported by DOE grant DE-ACO2-76SF00515 and NSF grants PHY-1002467 and DMR-0807731.

REFERENCES

- [1] Z. A. Conway, D. L. Hartill, H. S. Padamsee, and E. N. Smith. "Oscillating Superleak Transducers for Quench Detection in Superconducting ILC Cavities Cooled with He-II" Proc. of the LINAC08 Conf., Victoria, BC, Canada (2008)
- [2] C. C. Ackerman, B. Bertman, H. A. Fairbank, and R. A. Guyer, Phys. Rev. Lett. 16, (1996) 789.
- [3] J. Plouin, J.-P. Charrier, C. Magne, J. Novo, L. Maurice, "Experimental Investigations of the Quench Phenomena for the Quench Localization by the Second Sound Wave Method", Proc. Of the 2013 int. conf. on SRF, Paris, France (2013) 739.
- [4] S. Antipov et. al., "2D Simulation of Quench Dynamics", Fermilab Internal Report TD-11-017 (2011).
- [5] M. Fouaidy, F. Dubois, J.-M. Dufour, D. Longuevergne, A. Maroni, G. Michel, J.-F. Yaniche, "Calibration and Characterization of Capacitive OST

- Quench Detectors in SRF Cavities at IPN Orsay”, Proc. Of the 2013 int. conf. on SRF, Paris, France (2013) 714.
- [6] H. Padamsee, ”RF Superconductivity for Accelerators”, Wiley Publications, Weinheim
- [7] T. Bloomberg, “Heat Conduction in Two and Three Dimensions: Computer Modelling of Building Physics Applications”, Lund University Publications (1996).
- [8] B. Efrting, “Numerical calculations of thermal processes” The Swedish Council for Building Research (1990).
- [9] J. Vines et. al., “Systematic Trends for the Medium Field Q-Slope.” Proc. of the Int. Conf. on SRF, Beijing, China (2007).
- [10] A. Davies, “Material properties data for heat transfer modeling in Nb₃Sn magnets”, Illinois Accelerator Institute (2011) 17.
- [11] E. Koechlin, B. Bonin, “Parameterization of the niobium thermal conductivity in the superconducting state”, Superconducting Sci. Technol. 9 (1996).
- [12] B. J. Peters, “Advanced Heat Transfer Studies in Superfluid Helium for Large-scale High-yield Production of Superconducting Radio Frequency Cavities” Diploma Thesis, KIT Karlsruhe (2014).